

2-cm GPS altimetry over Crater Lake

Robert N. Treuhaft, Stephen T. Lowe, Cinzia Zuffada, and Yi Chao

Jet Propulsion Laboratory, California Institute of Technology, Pasadena, California

Abstract. Differences in electromagnetic path delay, between direct Global Positioning System (GPS) signals and those reflected from the surface of Crater Lake, have led to lake surface height estimates with 2-cm precision in 1 second. This is the first high-precision altimetric demonstration with GPS from sufficient altitude (≈ 480 m) to probe fundamental experimental errors, which bear on future air- and spaceborne passive GPS altimetry. It also serves as the first demonstration of a new approach to altimetric remote sensing in the coastal region, an area that is poorly measured by conventional radar altimetry. Time-series analyses suggest that tropospheric and thermal noise fluctuations dominate the altimetric error in this experiment. Estimating the differential delay from several simultaneously visible satellites may enable tropospheric error estimation and correction. Thermal noise on the reflected signal will be reduced with fully polarimetric observations and larger antenna apertures.

Introduction

The spatio-temporal structure of mesoscale eddies bears on ocean circulation and consequently on climate variability. These structures are unresolved in both space and time by current remote sensing techniques. Observations of sea surface temperature (e.g., from the Advanced Very High Resolution Radiometer [Cornillon *et al.*, 1987]) are frequently contaminated by clouds in the atmosphere, creating large spatial and temporal gaps in the remote sensing of temperature used to characterize eddies. Conventional satellite radar altimetry measures the sea surface height at high spatial resolution along its ground track (e.g., 7-km for TOPEX/Poseidon [Fu *et al.*, 1994]). However, the cross-track distance is usually quite large (e.g. on the order of 300 km for TOPEX/Poseidon). This spatial resolution, coupled with the 10-day repeat orbit of TOPEX/Poseidon, for example, is too coarse to monitor the evolution of ocean eddies. While the proposed wide-swath altimeter [Rodriguez *et al.*, 2001] will improve the spatial coverage, the temporal resolution is still 10 days, which is too long to track mesoscale ocean features.

Because Global Positioning System (GPS) signals are always globally present, and GPS receiver technology is inexpensive, the differential path delay of direct and ocean-reflected GPS signals, enabling passive altimetry from air- and spaceborne receivers, can potentially fill the spatio-temporal gaps of existing techniques [Martín-Neira *et al.*, 2001]. Coupling spaceborne GPS altimetry with conventional altimetry has the potential to greatly improve the

remote sensing of mesoscale eddies. Establishing an error budget for GPS altimetry requires diverse experiments, conducted with ground-based, airborne, and eventually spaceborne receivers. Experiments with ground-based receivers isolate errors due to atmospheric (if the receiver is high enough over the surface) and instrumental effects, as well as those due to surface roughness. Ground-based experiments turn off errors due to platform motion.

While previous reports of reception of ocean-scattered GPS signals have demonstrated low-altitude, ground-based altimetry [Martín-Neira *et al.*, 2000, 2001; Anderson, 1996], the first spaceborne detection (not altimetric) [Lowe *et al.*, 2001a], and the first airborne altimetry [Lowe *et al.*, 2000], this ground-based experiment, conducted at 480 m above Crater Lake in Oregon, probes atmospheric and instrumental effects. The Crater-Lake experiment isolated these two error sources, as surface roughness was not a big effect over the lake, and the scattered signal could be considered a coherent reflection. Quantifying these two basic error sources, which will affect all other types of GPS altimetry, is the first step in building an error budget.

In addition to beginning to establish the GPS altimetry error budget, this experiment demonstrates a cm-level phase measurement at low elevation angle from a fixed observation point, a technique which can potentially be applied to altimetry of the first 10-20-km of the coastal ocean. Continuous, high-accuracy GPS coastal altimetry will complement conventional altimetric sensors, the accuracy of which degrades near the coast.

Experiment geometry and data acquisition

The experiment at Crater Lake, in Central Oregon, was performed from the Cloudcap Lookout point about 480 m above the lake surface, as indicated in Figure 1. The fundamental observation for inferring the differential altitude of Cloudcap and the surface of Crater Lake is the difference in the propagation time of the reflected and direct signals. To sub-centimeter accuracy, this differential delay $\tau_{dif}(t, sat)$ at time t for a given satellite is the difference between the path length of the reflected signal, r_r , and the direct signal, r_d , divided by the speed of light, c , plus error terms:

$$\begin{aligned} \tau_{dif}(t, sat) &\equiv \frac{r_r - r_d}{c} + \epsilon_{cycle}(sat) + \epsilon(t, sat) \\ &= 2\frac{h}{c} \sin \theta(t, sat) + \tau_{curve}(\theta(t, sat)) \\ &+ \langle \tau_{zenith} \rangle m(\theta(t, sat)) + \epsilon_{cycle}(sat) + \epsilon(t, sat) \end{aligned} \quad (1)$$

where h is the differential altitude of the receiver and the lake surface. In (1), θ is the elevation angle of the GPS satellite above the local horizontal at the receiver, τ_{curve} is the delay correction due to Earth curvature (the first term

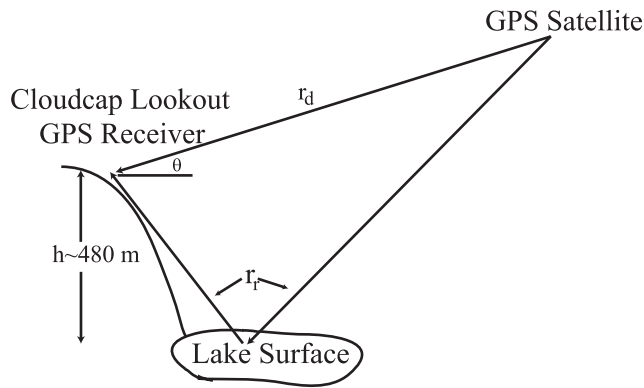


Figure 1. The geometry of the Crater Lake experiment from the Cloudcap Lookout. The direct path length from the satellite to the receiver is r_d . The arrows from r_r point to the two parts of the reflected path length.

alone describes the flat-Earth path delay), $\langle \tau_{zenith} \rangle$ is the average zenith tropospheric delay, and $m(\theta)$ is a function which, when multiplied by the zenith delay, gives the difference in tropospheric path delay between the reflected and direct signals. It is based on the mapping function of Niell, 1996. In (1), ϵ_{cycle} is an error equal to an integer number of GPS carrier wavelengths over the speed of light, because, as suggested below in (2), τ_{dif} is a phase delay determined only to a fraction of a GPS carrier cycle. In (1), ϵ is the delay error due to instrumental noise or unmodeled physical effects, such as tropospheric fluctuations. All time and satellite dependences are explicitly shown. An antenna was deployed with its axis pointing toward the lake, a few degrees below the horizontal, in order to receive both the direct and the reflected signals. Both signals were received at right-circular polarization, which is optimal for the direct signal and the reflected signal at very low elevations.

The raw analog GPS signal at the L-band carrier frequency, 1.57542 GHz, was frequency down-converted and digitized by the front end of a modified Turbo Rogue receiver [Meehan *et al.*, 1992], and a single channel was recorded using a Sony SIR-1000 recorder. The recorded signal, which contained both direct and reflected contributions, was cross correlated with reference functions in software [Lowe *et al.*, 2001b]. The amplitude and phase signatures in the cross correlation, due to interference of the direct and reflected signals, as a function of lag, were the principal observations from which τ_{dif} in (1) was estimated, as discussed in the next section.

Estimation of the differential delay

This section describes the estimation of the differential delay, from which (see (1)) the altitude of the receiver above the surface will be estimated. In order to estimate the differential delay, the cross correlation of the incoming signal containing the direct and reflected signals with reference functions is expressed in terms of τ_{dif} , as shown in (2). For reference functions offset by τ_i for the i^{th} lag, the complex cross correlation $\gamma(\tau_i)$ in the absence of cycle error and noise is:

$$\gamma(\tau_i) = e^{i\phi_0} \left[A_d \Lambda(\tau_i - \tau_0) \right.$$

$$\left. + A_r e^{ik_0(r_r - r_d)} \Lambda(\tau_i - \tau_0 - \frac{r_r - r_d}{c}) \right] \\ = e^{i\phi_0} \left[A_d \Lambda(\tau_i - \tau_0) + A_r e^{i\omega_0 \tau_{dif}} \Lambda(\tau_i - \tau_0 - \tau_{dif}) \right] \quad (2)$$

where ω_0 is the L-band angular carrier frequency, $2\pi \times 1.57542$ GHz, k_0 is the carrier wavenumber ω_0/c , and ϕ_0 is $k_0 r_d$ plus an arbitrary phase offset from the satellite. In (2), Λ is the triangular autocorrelation of the GPS code as a function of lag offset [Spilker, 1980], and τ_0 is the lag offset at the peak of the cross correlation function for the direct signal. The amplitude of the direct satellite signal is A_d , and A_r is the amplitude of the reflected signal, which depends on the product of the smooth-surface, Fresnel reflection coefficient (e.g. [Jackson, 1975]) and a term representing the amplitude loss of a coherently reflected wave due to surface roughness [Beckmann and Spizzichino, 1963; Miller *et al.*, 1984].

Eq. (2) shows that the complex cross correlation depends on the parameters τ_{dif} , A_d , τ_0 , A_r , and ϕ_0 . Standard approaches to nonlinear parameter estimation of geophysical parameters from remote sensing data (e.g. [Hamilton, 1964; Treuhaf and Siqueira, 2000]) were applied to estimate these five parameters for each 0.02-second data interval from a set of cross-correlation data from all lags (≈ 60 for the C/A code used) in which the signal is nonzero.

Altimetry results and errors

The altimetric parameter $h(t)$ is estimated from τ_{dif} using the model (2) for each time point (0.02 seconds apart) and satellite. A single $\langle \tau_{zenith} \rangle$ and an ϵ_{cycle} parameter for each satellite are estimated for a 12-minute interval using (1). The altimetric height parameter is allowed to vary with time and satellite to explore the altimetric error, and to facilitate estimating the other two parameters, which are derived under the constraint of making the slope of $h(t)$ as close to zero as possible. In order to determine $\langle \tau_{zenith} \rangle$ and ϵ_{cycle} , two sequences of τ_{dif} estimates from two different satellites were required. The satellites, identified by their pseudo-random-noise (PRN) number, were PRN 14 (7.5° to 11.2° elevation) and PRN 31 (23.8° to 20.1° elevation).

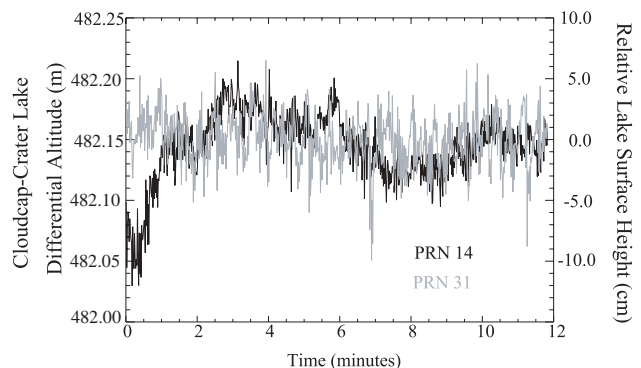


Figure 2. The differential altitude of the receiver at Cloudcap Lookout and the surface of Crater Lake, as determined from GPS reflection data from satellite PRN 14 (black) and PRN 31 (gray) at 1-second intervals. The right-hand ordinate shows the relative lake surface height, with 482.15 m subtracted from the lefthand ordinate. For 1-second data points rms height fluctuations were 2.8 and 2.1 cm for satellites PRN 14 and PRN 31, respectively. For 12-second data points, altimetric height fluctuations were 2.6 and 1.1 cm, respectively.

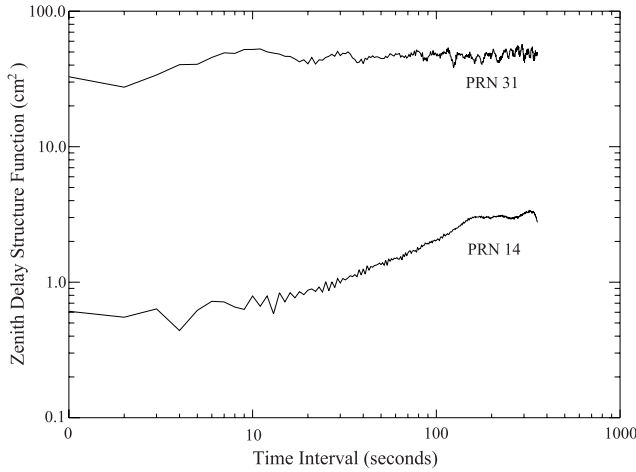


Figure 3. The structure functions of the zenith tropospheric delay as determined from PRN 14 and PRN 31.

Figure 2 shows the time series of the differential altitude of Cloudcap and the surface of Crater Lake, $h(t)$, for each satellite, for one-second averaging (fifty 0.02-second points). The right-hand ordinate shows the relative lake surface height. The caption indicates that approximately 2-cm precision was achieved in 1 second with the high-elevation PRN 31 alone, and less than 3 cm was achieved with PRN14 alone. The best-fit common zenith tropospheric delay parameter was 1.85 m light travel time, and the average heights from the two satellites agreed to within a few millimeters over the 12-minute span shown.

In order to derive an error budget for the fluctuations in $h(t)$ in Figure 2, a time-series analysis of the zenith tropospheric fluctuation [Treuhaft and Lanyi, 1987] was performed. The fluctuation, the difference between the actual effective zenith troposphere at time t and the average parameter estimated from the data, from (1), is

$$\begin{aligned} \tau_{zenith}(t) - \langle \tau_{zenith} \rangle &= \frac{h(t) - \langle h(t) \rangle}{m(\theta)} 2 \sin \theta \\ &\equiv \Delta \tau_{zenith}(t) \end{aligned} \quad (3)$$

where the brackets indicate ensemble average, but ergodicity is assumed and the time average of the height parameter is used, and $\Delta \tau_{zenith}$ is defined by (3). The structure function used to interpret the time series is defined as

$$\begin{aligned} \text{Structure Function}(T) &\equiv \\ &\langle (\Delta \tau_{zenith}(t+T) - \Delta \tau_{zenith}(t))^2 \rangle \end{aligned} \quad (4)$$

The structure function is flat as a function of the time interval argument T for white, uncorrelated noise, such as thermal instrumental noise. For tropospheric fluctuations, the structure function is proportional to T^α , where α is between $2/3$ and $5/3$ [Treuhaft and Lanyi, 1987]. The structure function of $\Delta \tau_{zenith}$ is shown in Figure 3, for satellites 14 and 31. It shows that the low-elevation PRN 14 tropospheric fluctuation has a slope of ≈ 0.75 for much of the spanned time intervals, consistent with tropospheric behavior. The higher-elevation PRN 31 fluctuation is seen to be flat, and is consistent with being dominated by thermal instrumental noise, and not by the troposphere.

Conclusions and the Impact of this Experiment on Future GPS Altimetry

A ground-based GPS altimetric experiment over Crater Lake yielded the first 2-cm-level precision at high receiver altitude. This first step in establishing an error budget for GPS altimetry suggested that tropospheric fluctuations and thermal instrumental noise dominated the altimetric error. Future ground-based experiments over the ocean will add the effects of ocean roughness to the error budget. Airborne experiments underway will further quantify errors associated with platform motion and a large footprint. Eventual spaceborne experiments will explore the effects of a much larger footprint.

In the analysis of this experiment, a physical model of the complex GPS cross correlation was used to extract the differential delay of the reflected and direct signal. The estimated differential delay depends on the altitude of the receiver above the water surface and other parameters. Height parameters were estimated for each of two GPS satellites. For 1-second averages, 2-cm precision was realized for the high-elevation-angle satellite. A single tropospheric parameter was estimated for the entire 12-minute interval, and a time-series analysis of fluctuations about that parameter suggested that the low-elevation satellite was dominated by tropospheric fluctuations, while the high-elevation satellite was dominated by thermal noise, most likely from the receiver.

Future air- and spaceborne GPS altimetry may benefit from the model-based approach to extracting the differential delay presented in this paper. For ocean applications, this model will have to be modified to include roughness corrections, perhaps with additional roughness parameters. Full polarimetric reception of the reflected signal will help future experiments of this type to increase the signal strength at higher elevation angles. Multiple satellite signals can potentially be used simultaneously in future demonstrations to reduce the effect of tropospheric fluctuations and thermal noise on the altimetric parameters.

Future ground-based deployments of GPS antennas and receivers will use the low-elevation interference signatures in this experiment over the ocean. Low-elevation, low-altitude (20-m) observations have been used to demonstrate local tide-gauge GPS applications [Anderson, 1996], but the high-altitude approach demonstrated here may enable coastal altimetry of the first 10-20 km, with very low elevation angles, perhaps of the order of 1 degree from coastal altitudes of, for example, 100-200 m. Current spaceborne altimeters do not sample frequently enough in space or time to track coastal features, which substantially evolve over the 10-day repeat cycle of spaceborne sensors over ≈ 10 -km spatial scales. The proposed low-elevation, ground-based altimetry will complement conventional radar altimetry in the coastal regions. The lower the elevation angle, the less the error due to surface roughness, enabling using the phase. But lower elevation observations suffer an increased error due to observation noise, from the $\sin \theta$ dependence in (1), and tropospheric fluctuations. Optimal operating elevations assessing these competing effects will have to be determined by experiment. We are currently analyzing data collected from a fixed-location GPS receiver deployed at an oil platform (height=40 m) off the California coast under the TOPEX/Poseidon ground track. This experiment should al-

low us to extend our results and understanding of the error budget from a lake environment to the open ocean. The ultimate goal is to make a direct comparison between GPS altimetry and TOPEX/Poseidon observations.

Acknowledgments. We thank Mark A. Smith for experiment deployment and Jesse Lerma of Sony Precision Technology America, Inc. for field deployment of the data recorder. The research described in this paper was carried out at the Jet Propulsion Laboratory, California Institute of Technology, under contract with the National Aeronautics and Space Administration (NASA).

References

- Anderson, K. D., A Global Positioning System (GPS) tide gauge, *Advisory Group for Aerospace Research and Development (AGARD), CP-582*, 1996.
- Beckmann, P. and A. Spizzichino, *The Scattering of Electromagnetic Waves from Rough Surfaces*, p. 81, Pergamon Press, Oxford, 1963.
- Cornillon, P., C. Gilman, C., L. Stramma, O. Brown, R. Evans and J. Brown, Processing and analysis of large volumes of satellite-derived thermal infrared data. *J. Geophys. Res.*, *92*, 12,993-13,002, 1987.
- Fu, L.-L., E.J. Christensen, C.A. Yamarone Jr., M. Lefebvre, Y. Menard, M. Dorrer, and P. Escudier, TOPEX/Poseidon Mission Overview. *J. Geophys. Res.*, *99*, 24,369-24,381, 1994.
- Hamilton, W. C., *Statistics in Physical Science: Estimation, Hypothesis Testing, and Least Squares*, pp. 150-156, Ronald Press Company, New York, 1964.
- Jackson, J. D., *Classical Electrodynamics*, pp. 278-282, Wiley & Sons, Inc., New York, 1975.
- Lowe, S. T., C. Zuffada, J. L. LaBrecque, M. F. Lough, J. Lerma, and L. E. Young, An ocean-altimetry measurement using reflected GPS signals from a low-altitude aircraft, IGARSS 2000, Honolulu, HI, 24-28 July, 2000.
- Lowe, S. T., J.L. Labrecque, C. Zuffada, L.J. Romans, L. Young and G. A. Hajj, First spaceborne observation of an earth-reflected GPS signal, *Radio Sci.*, in press, 2001a.
- Lowe, S. T., P. M. Kroger, G. W. Franklin, J. L. LaBrecque, J. Lerma, M. F. Lough, M. R. Marcin, D. J. Spitzmesser, L. E. Young, A delay/Doppler-mapping receiver system for GPS-reflection remote sensing, *IEEE Trans. on Geosci. and Remote Sensing*, in review, 2001b.
- Martin-Neira, M., M. Caparrini, J. Font-Rossello, S. Lannelongue, and C. Serra Vallmitjana, The PARIS Concept: An Experimental Demonstration of Sea Surface Altimetry Using GPS Reflected Signals, *IEEE Trans. Geosci. and Remote Sensing*, *39*, 142-150, 2001.
- Martin-Neira, M., P. Colmenarejo, G. Ruffini, C. Serra, Ocean Altimetry Using The Carrier Phase Of GnsS Reflected Signals, *Cersat Journal, Issue 11, Scientific Topic No.22*, 2000.
- Meehan, T. K., C.B. Duncan, C.E. Dunn, T.N. Munson, D.J. Spitzmesser, J.M. Srinivasan, J.Y. Tien, J.B. Thomas., The TurboRogue receiver, *Sixth International Geodetic Symposium on Satellite Positioning*, Columbus, Ohio, 209-218, 1992.
- Miller, A.R., R.M. Brown, and E. Vegh, New derivation for the rough surface reflection coefficient and for the distribution of sea-wave elevations, *IEEE Proceedings*, *131*, 114-116, 1984.
- Niell, A. E., Global mapping functions for the atmosphere delay at radio wavelengths *J. Geophys. Res., -Solid Earth*, *101*, B2, 3227-3246, 1996.
- Rodriguez, E., B. D. Pollard, and J. M. Martin, Wide-swath ocean altimetry using radar interferometry, *IEEE Trans. on Geosci. and Remote Sensing*, in press, 2001.
- Spilker, J. J., GPS signal structure and performance characteristics, *Global Positioning System, Papers Published in Navigation 1*, edited by P. M. Janiczek, pp. 29-54, The Institute of Navigation, Washington, D. C., 1980.
- Treuhaft, R. N., and G. E. Lanyi, The effect of the dynamic wet troposphere on radio interferometric measurements, *Radio Sci.*, *22*, 251-265, 1987.
- Treuhaft, R. N. and P. R. Siqueira, Vertical structure of vegetated land surfaces from interferometric and polarimetric radar, *Radio Sci.*, *35*, 141-177, 2000.

R. Treuhaft, S. Lowe, C. Zuffada, Y. Chao, Jet Propulsion Laboratory, California Institute of Technology, 4800 Oak Grove Drive, MS 138-212, Pasadena, CA 91109. (e-mail: Robert.Treuhaft@jpl.nasa.gov; Stephen.Lowe@jpl.nasa.gov; Cinzia.Zuffada@jpl.nasa.gov; Yi.Chao@jpl.nasa.gov)

(Received July 20, 2001; accepted September 6, 2001.)